

# Assessing CO<sub>2</sub> fluxes during enhanced weathering from soils through a mesocosm lens

Isabella Chiaravalloti<sup>1\*</sup>, Shuang Zhang<sup>2</sup>, and Noah J. Planavsky<sup>1,3</sup>

<sup>1</sup> Department of Earth and Planetary Sciences, Yale University, New Haven, CT, United States

<sup>2</sup> Department of Oceanography, Texas A&M University, College Station, TX, United States

<sup>3</sup> Yale Center for Natural Carbon Capture, Yale University, New Haven, CT, United States

\* Author to whom any correspondence should be addressed.

Email: isabella.chiaravalloti@yale.edu

## Abstract

It is becoming increasingly accepted that annual gigatonne-scale CO<sub>2</sub> removal, in conjunction with rapid decarbonization, is necessary to meet international climate goals and limit global warming below 2°C. This is going to require the development and rapid scaling of new forms of carbon management. When developing new CDR techniques, it is essential to ensure that there is complete accounting of how the process affects greenhouse gas fluxes. Enhanced weathering (EW), the spreading of finely ground alkaline minerals to soils, has the potential to sequester significant amounts of CO<sub>2</sub> while improving soil health. However, its effects on soil organic carbon (SOC) decomposition and CO<sub>2</sub> efflux from soils remain debated. It has been proposed that increasing soil pH can lead enhanced SOC remineralization. To move forward this debate, we present CO<sub>2</sub> flux and soil carbon pool data from a greenhouse study in large mesocosms. We focused on mildly acidic soil in which the majority of cations from weathering would move into the exchangeable fraction in soils. Therefore, gas fluxes changes should be largely linked to changes in SOC stores. We find no significant correlation between CO<sub>2</sub> fluxes and soil pH and no significant correlation between CO<sub>2</sub> fluxes and basalt application. Although this does not rule out a link between soil pH and SOC remineralization rates, the effect is small relative to other factors, like temperature and soil moisture. Although minor increases in total inorganic carbon were observed in basalt-amended soils, these increases did not support a direct link between soil pH and increased CO<sub>2</sub> emissions. We observed a small increase in soil total organic carbon stocks, but this change was also not significant enough to drive a shift in observed soil CO<sub>2</sub> fluxes.

Keywords: Enhanced weathering, soil organic carbon, CO<sub>2</sub>, carbon dioxide removals

## Introduction

Combating climate change will require carbon dioxide removal (CDR) strategies in addition to aggressive and rapid emissions reductions to meet climate goals (1). Pathways suggest that we need annual gigatonne scale CO<sub>2</sub> removal to limit our average global warming to below 2°C even

with optimistic emissions reduction scenarios (1–3). However, because there are still real shortcomings in our ability to evaluate the effects and the effectiveness of most forms of CDR — especially open system interventions — there is an obvious impetus to improve our understanding of potentially promising pathways of CDR (4–7).

Enhanced weathering (EW) is one of these potentially promising CDR technologies that has seen a recent upswing in interest, basic research, and commercialization. EW, the application of finely ground cation-rich rocks or minerals to soils, captures CO<sub>2</sub> as the minerals dissolve (7–11). This strategy has been proposed to be capable of capturing 0.5–2 gigatonnes of CO<sub>2</sub> per year (12) — although from a geochemical standpoint, this number could be much higher (13–15). Most emphasis to date has been upon finely ground silicate minerals - however a wide range of feedstocks, including carbonates, slag, and cement waste, could, in theory, be utilized (12,16–19). Upon dissolution, alkaline minerals consume protons and release base cations, which increases the pH of the soil system. Decreasing soil acidification commonly improves soil conditions for crop growth and nutrient bioavailability (9,11). EW can also release micronutrients such as calcium, magnesium, potassium, phosphorus, silicon, copper, zinc, manganese, and iron that can improve soil health and crop yield (20–26).

A potential negative compounding effect, however, is that EW may stimulate the rate of decomposition of soil organic carbon (SOC) by increasing soil pH, thereby increasing the release of CO<sub>2</sub> from soils. Some liming studies have found that pH significantly alters net carbon mineralization and primes carbon by altering soil microbiota (27); however, this enhancement of SOC mineralization may be temporary and is often followed by increases in SOC stocks (28). Small scale mesocosms (10L) have suggested that basalt can drive a temporary initial CO<sub>2</sub> release — presumably from increased SOC decay as soil pH increases, and this varies by soil type (29). A wollastonite mesocosm study indicates that EW increases SOC mineralization and therefore CO<sub>2</sub> efflux, potentially by increasing the availability of nutrients that stimulate microbial decomposition via release of silicon and/or by increasing soil pH (30). However, this is contrasted by another mesocosm study, in which there was no difference in CO<sub>2</sub> respiration between control and olivine amended incubated soils (31). Several studies have also suggested that EW may stabilize SOC, as they found increases in mineral-associated organic matter in EW treated soils (32,33). The variability in findings regarding SOC and CO<sub>2</sub> flux responses underscores the need for further investigation into whether EW alters SOC dynamics in order to better understand its implications for CDR.

SOC pools are a continuum, with varying levels of recalcitrance, and therefore have different sensitivities to levers on decomposition, such as temperature dependence of enzymes, soil moisture, soil mineralogy, and soil structural stability and aggregates (34–36). Decomposition pathways are sensitive to each soil system (35). There is agreement that temperature influences the rate of organic decay by stimulating microbial activity and respiration (34,37). However, the rates of decay of recalcitrant SOC pools may be more sensitive to temperature than those of more labile forms of SOC (34). Soil moisture also plays a large role in carbon cycling as increases in soil moisture (particularly after rewetting events) tend to increase microbial activity, and therefore respiration (38). However, the relationship between SOC and soil moisture is nuanced, variable, and still debated (39). There are likely confounding effects between soil moisture and its effect on the temperature coefficient (Q<sub>10</sub>) for SOC decomposition (39,40). Organic matter is more

protected within aggregates, and perturbations to the soil structure, such as tillage, will therefore alter SOC remineralization rates (36,41–44). Simultaneously controlling all these variables while mimicking field conditions presents a challenge for experimental work monitoring SOC decomposition rates.

Experiments under controlled conditions—greenhouse and growth chamber experiments—provide one way to facilitate a controlled, well monitored system where it is possible to try to interrogate the links between organic carbon remineralization rates, soil pH and EW (45–47). However, reproducible experiments in controlled systems can be hard to be generate. Temperature can vary widely between mesocosms even in well maintained greenhouses due to uneven overhead lighting and air circulation; these differences may alter the relative humidity and evapotranspiration rates in each container (45–47). Humidity can dramatically alter photosynthesis rates by influencing the aperture of stomata and their conductance (48–51). However, randomizing the experimental layout to evenly distribute the unwanted variation can decrease erroneous positive correlation between groups (45–47). Further, smaller column style experiments are not ideally suited for EW SOC analyses because they are subject to artifacts and edge effects (i.e., sidewall flow, particularly in unsaturated columns but also in packed columns (52)) and are more variable to changes in soil moisture and temperature. Smaller pots can restrict plant growth, particularly if roots are impacted, which can hamper plant uptake of water and nutrients (53). It is also important to source soil for these experiments scientifically responsibly — soil microbial communities vary by plant type, soil chemistry, and spatial location, and soil sourced from a location that is not representative of the desired system may behave differently than a more optimal choice (53,54). This is particularly important for experiments investigating variables that are heavily influenced by microbial activity (i.e., SOC decomposition). As SOC is sensitive to soil texture, using natural soils is preferred to potting soils, that aren't representative of natural microbial communities, don't have characteristic soil structure, and don't retain nutrients as well as do natural soils (53). Building from this foundation, we conducted large mesocosm experiments, designed to explore the role that basalt addition will have on SOC dynamics.

Specifically, here we present carbon stock and CO<sub>2</sub> flux data generated from a series of EW experiments performed in large mesocosms in a greenhouse (55). We used large 121-liter mesocosms to minimize edge effects and to ensure adequate volume of soil for corn root depth. We use roughly an order of magnitude more soil (sourced from an organic working farm) than in previous EW studies (25,30,56–59), and we performed continuous monitoring of multiple environmental factors. We also intentionally designed the layout of the containers to decrease unintentional spatial correlations. We conducted experiments in an acidic soil where the short term CO<sub>2</sub> removal flux from weathering will be delayed due to cation sorption (60). This allows us to provide another perspective on whether EW increases, maintains, or decreases the rate of SOC remineralization, CO<sub>2</sub> efflux, and size of SOC stocks.

## **Methods**

In two sequential mesocosm experiments (Run 1 and Run 2), we grew maize (*zea mays*, Reid's Yellow Dent Open Pollinated Corn Seed, Bradley Seed Brand) in soils that had been amended with fine grained basalt in a research greenhouse, as used in (55). The experimental design was previously described by (55) and therefore is only summarized in Supplementary Table 1. The

containers in these two experiments had basalt tilled into the soil at the beginning of Run 1; after harvesting, we began Run 2 by planting maize on the same soil, thereby treating Run 2 as a second growth season on a previously amended “field”. A key point of the experimental design was that this research greenhouse was equipped with an automated watering system to ensure that all pots received the same amount of water at the same time. The greenhouse was set to a specific day (28°C) and night (17°C) temperature and contained fan coil units to evenly distribute the air in the room. Furthermore, the treatments were distributed throughout the room to minimize artifacts from temperature and humidity gradients. The chosen containers were specifically selected to be deep enough for corn roots for the duration of the experiment (61), and also abide by the minimum recommended diameter to length ratio (1:4) for good column experiment practices put forth by (52).

Throughout the duration of these experiments, we took weekly measurements of topsoil pH, topsoil buffer pH (using the Sikora buffer), as well as pore water alkalinity (using Rhizon samplers) and soil moisture with a Spectrum Technologies TDR 150 soil moisture meter (accuracy of  $\pm 3.0\%$  VWC) at three depths (15 cm, 35 cm, and 50 cm) (55). Alkalinity was calculated using 0.0501N HCl as a titrant and a Thermo Scientific Orion Star T920 redox titrator which was determined to have an error of 1.4% based on the 4mL sample size (55). We also continuously measured CO<sub>2</sub> fluxes and temperature at soil surface using Eosense automated soil flux chambers paired with a G2508 Picarro Cavity Ringdown Spectrometer (62–64). The 1 $\sigma$  precision for CO<sub>2</sub> measurements is <600 ppb + 0.05% of reading.

We also measured total carbon (TC) and total inorganic carbon (TIC) from soil samples that were scooped from the surface (between 0-4cm). These samples were stored frozen at -20°C and then dried at 65°C then ground via mortar and pestle to achieve a fine powder prior to analysis. To determine the carbon stocks, we performed combustion in an induction furnace (TC) and acid dissolution (TIC) followed by measurement of released carbon dioxide on an Eltra CS 580 Carbon Sulfur Determinator. Total organic carbon (TOC) was calculated by subtracting TIC from TC. This instrument measured standards to within 1.55% of the measured TC standard (Eltra GmbH 90817, 2.05% carbon) and within 1.75% of the measured TIC standard (Alpha Resources AR4029, 4.93% carbon).

All data analysis followed the methods used in (55). In summary, the flux measurements were integrated in Python to calculate total emissions, and a two-tailed t-test function was used to test for the difference between means of cumulative emissions. In R, a random forest algorithm (using 75% of the data on the training dataset, and 25% on the test dataset) followed by the permutation method was used to ensure that all necessary variables were measured to successfully predict the CO<sub>2</sub> flux and to assess the relative importance of each variable (pH, buffer pH, temperature, soil moisture (at each depth), photosynthetically active radiation (PAR), and time) on the CO<sub>2</sub> flux. All standard deviations of the group represent 1 $\sigma$  precision. We opted to use a rolling 48-hour average for temperature to avoid confounding effects of diurnal temperature and PAR as the climate was set to have cooler temperatures at night when the lights were set to be off (and hotter temperatures during the day when the lights were on).

## **Results**

### *1.1 Run 1*

The experiment duration for Run 1 was 24 days. In Run 1, the basalt amended containers on average had higher CO<sub>2</sub> emissions than the control containers, but there was no statistically significant difference between them (Figure 1, Table 1, Table 2). The CO<sub>2</sub> flux results from Run 1 did not reject the null hypothesis (i.e., there was no difference between the control and treatment). As described in (55), both the buffer pH and the soil pH were higher (0.46 and 1.1 pH units higher, respectively) in the basalt amended containers than the control containers, and both temperature and soil moisture varied between containers. The changes in alkalinity were not statistically significant, however, the basalt amended containers had higher alkalinity values on average at all depths measured (with differences of 134 μmol/L, 31 μmol/L, and 305 μmol/L at 15 cm, 35 cm, and 50 cm, respectively) (55). Despite the high-performance climate control of the greenhouse and the automated watering system, the containers experienced consistent differences in temperature due to spatial heterogeneity in the greenhouse, and unpredictable differences in soil moisture (Supplementary Figure 1 and Supplementary Figure 2).

When performed on the results from Run 1, the machine learning framework yielded an R<sup>2</sup> of 0.99 for the training data and 0.91 for the test data (Supplementary Figure 3). The permutation importance technique indicated that the strongest levers on CO<sub>2</sub> fluxes were time and amount of PAR (Supplementary Figure 4b); they were negatively correlated with CO<sub>2</sub> flux (Supplementary Figure 4a) likely due to more plant growth as time goes on and with more light. Soil moisture at the middle of the column (35cm) was the next strongest lever on CO<sub>2</sub> fluxes, then soil moisture at depth (50cm), soil pH, buffer pH, 48-hour average temperature, and lastly surface soil moisture (15cm) (Supplementary Figure 4b). There were no obvious correlations between CO<sub>2</sub> flux and pH (Figure 1), however, based on the Spearman's rank correlation, pH had a slightly negative correlation with CO<sub>2</sub> fluxes (Supplementary Figure 4a).

### *1.2 Run 2*

The experiment duration for Run 2 was 29 days. In Run 2, the basalt amended containers had lower CO<sub>2</sub> emissions than the control containers, but there was no statistically significant difference between them (Figure 2, Table 1, Table 2). Both the buffer pH and the soil pH remained higher in the basalt amended containers than the control containers, and both temperature and soil moisture varied between containers (Supplementary Figure 1) (55).

The machine learning framework yielded an R<sup>2</sup> of 0.99 for the training data and 0.93 for the test data on Run 2 (Supplementary Figure 5). For this run, the permutation importance technique indicated that the strongest lever on CO<sub>2</sub> fluxes was the amount of PAR; this was again negatively correlated with CO<sub>2</sub> flux (Supplementary Figure 6). Soil moisture at the middle of the column (35cm) was indicated as the next strongest lever on CO<sub>2</sub> fluxes and was positively correlated (Supplementary Figure 6). Time, then surface soil moisture (15cm), buffer pH, soil pH, soil moisture at depth (50cm), and finally 48-hour average temperature were the next strongest levers on CO<sub>2</sub> fluxes (Supplementary Figure 6b). Again, pH had a slightly negative correlation with CO<sub>2</sub> fluxes, based on the Spearman's rank correlation (Supplementary Figure 6a).

### *1.3 Runs 1 and 2 Data Compared and Combined*

Between the two iterations of the experiment, the average CO<sub>2</sub> flux switched from being higher to lower (when basalt amended mesocosms are compared to control mesocosms), and, in neither of these cases was this difference statistically significant based on a t-test (Figure 3a, Figure 3c, Table 1, Table 2). The standard deviation of these measurements was between 14% and 46% of the average values. We also saw no obvious correlation between CO<sub>2</sub> flux and soil pH; when a linear regression was performed on the combined data from Run 1 and Run 2, it revealed an R<sup>2</sup> of 0.00 (Figure 4).

When performed on the data from Run 1 and then Run 2, a bootstrap resampling (n=1000) indicated a switch in which type of container had a higher CO<sub>2</sub> flux. There was no overlap of the basalt and control peaks within 95% confidence intervals in either run, and the average value fell within each respective 95% confidence interval (Figure 3b, Figure 3d). We then performed bootstrap resampling analysis on the combined datasets of Run 1 and Run 2; this showed overlaps in the confidence intervals between the two distributions meaning that there was no difference between the distributions when combined (Figure 3e, Figure 3f).

We then ran the combined data from Run 1 and Run 2 on the machine learning framework. It yielded an R<sup>2</sup> of 0.99 for the training data and 0.93 on the test data (Supplementary Figure 7). For the combined runs, the permutation importance technique indicated that the strongest lever on CO<sub>2</sub> fluxes was time and then the amount of PAR (Figure 5). The next strongest lever on CO<sub>2</sub> fluxes was soil moisture at the middle of the column (35cm) (Figure 5). The next strongest levers on CO<sub>2</sub> fluxes are listed in order of decreasing importance: buffer pH, soil moisture at depth (50cm), surface soil moisture (15cm), soil pH, and lastly 48-hour average temperature (Figure 5). The minimal influence of soil pH on CO<sub>2</sub> fluxes is further supported by the random forest machine learning framework, which identified time, PAR, and soil moisture as more significant factors affecting CO<sub>2</sub> flux compared to soil pH in both iterations of the experiment. Because plants grow with time, and perform more photosynthesis with more PAR, it makes sense that these were the dominant levers on CO<sub>2</sub> fluxes. Temperature was identified as the least important variable, however, that is likely because we used the rolling average temperature over a 48-hour period to deconvolve the effects of PAR and diurnal temperature, and because we explored a small temperature range.

#### *1.4 Effects of Data Pruning*

To assess the effects of more intermittent sampling, we randomly removed 50% and 90% of the data from the combined dataset of Runs 1 and 2 and took the average of those values 100 times. We show the distribution of differences between the control and basalt average CO<sub>2</sub> flux value for each of these re-samplings in Figure 6. We found that this can cause shifts in the sign of the difference in flux (i.e., whether the control or the basalt amended mesocosms had higher CO<sub>2</sub> fluxes). While there is no statistically significant difference between these two distributions (p-value = 0.80), and the true mean overall difference between control and basalt (0.02 μmol/m<sup>2</sup>s) falls between the 95% confidence intervals of both these distributions, both the range and the 95% confidence intervals are much wider in the 90% removed distribution than the 50% removed distribution (Supplementary Table 2). This highlights the need for continuous or high frequency sampling as lower frequency sampling may obscure the signal and lead to incorrect conclusions about relative gas flux magnitudes.

### 1.5 Soil Carbon Stocks

Run 1 and Run 2 are combined to create a time series of the soil carbon stocks through time, and the values from control and basalt amended containers are compared (Figure 7). In all cases, the basalt amended containers had higher average TOC than the control containers (Table 3, Figure 7). However, this was only statistically significant on date 08/01/2022, and when all post-amended timestamps (all dates except 07/27/2022) are clustered (Table 5).

With respect to TIC, basalt amended containers had on average more than control containers on all dates post application (Supplementary Table 3, Figure 7). This was statistically significant for all post application dates and the combined post application dates (Table 5). Pre-application-of-basalt, all containers had TIC values below detection limits, indicating that a small amount of carbonate precipitation occurred during the experiment due to the rise in the soil pH as EW occurred (Supplementary Table 3), supporting the findings of (65).

Basalt amended containers had on average more TC than control containers on all dates (Table 4, Figure 7). This was statistically significant only for the date 08/01/2022 and for the combined post-amendment timestamps (Table 5).

### Discussion

Although there is a signal for a significant pH shift with basalt addition, there was no sign of a significant shift in the CO<sub>2</sub> fluxes in modified mesocosms. Given there was no significant evidence for increased alkalinity fluxes in this system, the cations released during weathering are moving on exchange sites in the soil column and/or being consumed as carbonates precipitate (as evidenced by the small but statistically significant increase in TIC in basalt amended containers). Given strong effects of cation sorption, despite weathering, gas fluxes are controlled by CO<sub>2</sub> fluxes. Therefore, this work provides no support for the hypothesis that, in typical agronomic conditions (not extremely acidic soils), EW will increase SOC degradation rates. This is noteworthy given that these are large mesocosms in a controlled setting with continuous CO<sub>2</sub> monitoring that, arguably, provide the most comprehensive look at this process.

However, this work also stresses the difficulty of using soil CO<sub>2</sub> fluxes to accurately track SOC remineralization. Our factor analysis suggests multiple parameters (e.g., soil moisture) play a more important role in controlling CO<sub>2</sub> fluxes than pH. In multiple iterations of the same experiment, there was a switch in which treatment emitted more cumulative CO<sub>2</sub> emissions on average, caution should be exercised when linking flux to pH. Taken alone, each iteration of the experiment can lead to the drawing of opposite conclusions. Although these trends are not significant, this is an indication of difficulty of tracking carbon fluxes with CO<sub>2</sub> fluxes. Nonetheless, our results could be consistent with the soil priming findings of (27–29), we observed a higher CO<sub>2</sub> flux in basalt amended containers in Run 1 of the experiment, but lower CO<sub>2</sub> fluxes from basalt amended containers in Run 2 of the experiment. This study benefits from continuous monitoring of levers and fluxes, and yet, the high variability in CO<sub>2</sub> fluxes within each treatment on homogeneous soil compositions demonstrates the difficulty of accurately measuring changes in CO<sub>2</sub> flux. These fluxes are incredibly variable and sensitive, resulting in a low signal to noise ratio. Non-continuous

sampling will be even less representative of the system. This suggests that periodic gas flux sampling (particularly for gases with small magnitudes of fluxes or with small signal to noise ratios) is unlikely to yield meaningful data on the effects of EW on carbon fluxes. We hope that these results can be used to help design experiments that depend on intermittent bottle fluxes or eddy covariance approaches that may lead to signals from different portions of the monitoring area depending on the prevailing winds.

Furthermore, this work suggests that if conclusions are going to be drawn about changes in CO<sub>2</sub> efflux, it is critical that all relevant variables are monitored. Without synchronized data on soil moisture, which is spatially heterogeneous even in a highly controlled environment, it is impossible to make meaningful inferences about CO<sub>2</sub> data. It is evident from prior studies that soil moisture and soil texture are key players in CO<sub>2</sub> flux and SOC remineralization (34–36,38,39,41–44,66), and these two levers are heavily influenced by agricultural practices. These factors, along with soil structure, will be difficult to constrain in many experimental settings. In particular, in smaller mesocosms that are subject to edge effects and irregular soil packing, these effects will likely be difficult to control.

We found statistically higher TOC and TIC (and therefore, TC) values in basalt amended containers post-amendment. In particular, the minor increase in TOC (between 0.08 and 0.28% higher) could indicate a co-benefit of EW causing an increase in SOC storage. We attribute the slight increase in TIC to carbonate precipitation. These two fluxes changes would offset each other from a gas flux perspective—carbonate precipitation will foster CO<sub>2</sub> evasion. However, caution is needed in any conclusions about soil TOC and TIC values, given we are measuring carbon stocks from surface level samples.

## **Conclusions**

Greenhouse studies, such as this one, can remove variability that is present in field conditions to perform a closer examination of relationships between perturbations in soil systems. We present results from an experiment designed to allow for dissolution of basalt feedstock but limited transport of weathering products from the system. There is clear evidence of weathering — foremost in strong increases in soil pH and percent base saturation. However, there is no evidence for increased alkalinity fluxes from the system. Therefore, in these experiments, the gas fluxes from the top of the soil column are controlled by shifts in organic matter storage. We did not observe any significant changes in CO<sub>2</sub> fluxes between basalt amended and control mesocosms. This clashes with the idea that EW and increases in soil pH will lead to loss of SOC.

## **Acknowledgements**

This research made use of the Yale Analytical and Stable Isotope Center at Yale University. We would also like to acknowledge Brad Erkkila for his staff expertise and assistance with the Eltra CS 580 Carbon Sulfur Determinator. This research made use of the Yale Science Building research greenhouses within Yale University's Marsh Botanical Gardens plant growth facility. We would like to acknowledge Christopher Bolick and Nathan Guzzo for their staff expertise and assistance with the Argus control systems. We would like to thank Nicolas Theunissen for assistance with figure creation.



## Funding

The authors declare that this study received funding from the Yale Center for Natural Carbon Capture. The funder was not involved in the study design, collection, analysis, interpretation of data, the writing of this article, or the decision to submit it for publication.

## References

1. IPCC. Climate Change 2022: Impacts, Adaptation and Vulnerability. Working Group II Contribution to the Sixth Assessment Report of the Intergovernmental Panel on Climate Change. Cambridge University Press, Cambridge, UK and New York, NY, USA: Cambridge University Press; 2022 p. 3056.
2. Rogelj J, Shindell D, Jiang K, Fifita S, Forster P, Ginzburg V, et al. Mitigation Pathways Compatible with 1.5°C in the Context of Sustainable Development in In: Global Warming of 1.5°C. An IPCC Special Report on the impacts of global warming of 1.5°C above pre-industrial levels and related global greenhouse gas emission pathways, in the context of strengthening the global response to the threat of climate change, sustainable development, and efforts to eradicate poverty [Masson-Delmotte, V., P. Zhai, H.-O. Pörtner, D. Roberts, J. Skea, P.R. Shukla, A. Pirani, W. Moufouma-Okia, C. Péan, R. Pidcock, S. Connors, J.B.R. Matthews, Y. Chen, X. Zhou, M.I. Gomis, E. Lonnoy, T. Maycock, M. Tignor, and T. Waterfield (eds.)]. [Internet]. 1st ed. Cambridge University Press; 2018 [cited 2024 Sep 26]. Available from: <https://www.cambridge.org/core/product/identifier/9781009157940/type/book>
3. Vaughan N, Fuss S, Buck H, Schenuit F, Pongratz J, Schulte I, et al. The State of Carbon Dioxide Removal - 2nd Edition. 2024 [cited 2024 Nov 18]; Available from: <https://osf.io/f85qj/>
4. CarbonPlan and Frontier. CarbonPlan. 2023 [cited 2024 Nov 18]. CDR Verification Framework — methods. Available from: <https://carbonplan.org>
5. Lebling K, Riedl D, Leslie-Bole H. Measurement, Reporting, and Verification for Novel Carbon Dioxide Removal in US Federal Policy. WRIPUB [Internet]. 2024 Jun [cited 2024 Nov 18]; Available from: [https://www.wri.org/research/measurement-reporting-and-verification-novel-carbon-dioxide-removal?auHash=rLtKBvDkX0auKYcYp\\_RiaIDTlpxQAly2kLH21DTMNZs](https://www.wri.org/research/measurement-reporting-and-verification-novel-carbon-dioxide-removal?auHash=rLtKBvDkX0auKYcYp_RiaIDTlpxQAly2kLH21DTMNZs)
6. Tao F, Houlton BZ. Inorganic and organic synergies in enhanced weathering to promote carbon dioxide removal. *Global Change Biology*. 2024 Jan;30(1):e17132.
7. Vandeginste V, Lim C, Ji Y. Exploratory Review on Environmental Aspects of Enhanced Weathering as a Carbon Dioxide Removal Method. *Minerals*. 2024 Jan 8;14(1):75.
8. Abdalqadir M, Hughes D, Rezaei Gomari S, Rafiq U. A state of the art of review on factors affecting the enhanced weathering in agricultural soil: strategies for carbon sequestration and climate mitigation. *Environ Sci Pollut Res*. 2024 Feb 19;31(13):19047–70.
9. Beerling DJ, Leake JR, Long SP, Scholes JD, Ton J, Nelson PN, et al. Farming with crops and rocks to address global climate, food and soil security. *Nature Plants*. 2018 Mar;4(3):138–47.

10. Fawzy S, Osman AI, Doran J, Rooney DW. Strategies for mitigation of climate change: a review. *Environ Chem Lett*. 2020 Nov 1;18(6):2069–94.
11. Renforth P. The potential of enhanced weathering in the UK. *International Journal of Greenhouse Gas Control*. 2012 Sep 1;10:229–43.
12. Beerling DJ, Kantzas EP, Lomas MR, Wade P, Eufrazio RM, Renforth P, et al. Potential for large-scale CO<sub>2</sub> removal via enhanced rock weathering with croplands. *Nature*. 2020 Jul 1;583(7815):242–8.
13. Baek SH, Kanzaki Y, Lora JM, Planavsky N, Reinhard CT, Zhang S. Impact of Climate on the Global Capacity for Enhanced Rock Weathering on Croplands. *Earth's Future*. 2023;11(8):e2023EF003698.
14. Strefler J, Amann T, Bauer N, Kriegler E, Hartmann J. Potential and costs of carbon dioxide removal by enhanced weathering of rocks. *Environ Res Lett*. 2018 Mar;13(3):034010.
15. Zhang S, Planavsky NJ, Katchinoff J, Raymond PA, Kanzaki Y, Reershemius T, et al. River chemistry constraints on the carbon capture potential of surficial enhanced rock weathering. *Limnology & Oceanography* [Internet]. 2022 Nov [cited 2023 Jan 22];67(S2). Available from: <https://onlinelibrary.wiley.com/doi/10.1002/lno.12244>
16. Chukwuma JS, Pullin H, Renforth P. Assessing the carbon capture capacity of South Wales' legacy iron and steel slag. *Minerals Engineering*. 2021 Nov;173:107232.
17. Knapp WJ, Stevenson EI, Renforth P, Ascough PL, Knight ACG, Bridgestock L, et al. Quantifying CO<sub>2</sub> Removal at Enhanced Weathering Sites: a Multiproxy Approach. *Environ Sci Technol*. 2023 Jul 4;57(26):9854–64.
18. Renforth P, Washbourne CL, Taylder J, Manning DAC. Silicate Production and Availability for Mineral Carbonation. *Environ Sci Technol*. 2011 Mar 15;45(6):2035–41.
19. Knapp WJ, Tipper ET. The efficacy of enhancing carbonate weathering for carbon dioxide sequestration. *Front Clim*. 2022 Aug 11;4:928215.
20. Anda M, Shamshuddin J, Fauziah CI. Improving chemical properties of a highly weathered soil using finely ground basalt rocks. *CATENA*. 2015 Jan;124:147–61.
21. Beerling DJ, Epihov DZ, Kantola IB, Masters MD, Reershemius T, Planavsky NJ, et al. Enhanced weathering in the US Corn Belt delivers carbon removal with agronomic benefits. *Proceedings of the National Academy of Sciences*. 2024 Feb 27;121(9):e2319436121.
22. Guo F, Wang Y, Zhu H, Zhang C, Sun H, Fang Z, et al. Crop productivity and soil inorganic carbon change mediated by enhanced rock weathering in farmland: A comparative field analysis of multi-agroclimatic regions in central China. *Agricultural Systems*. 2023 Aug;210:103691.
23. Kantola IB, Masters MD, Beerling DJ, Long SP, DeLucia EH. Potential of global croplands and bioenergy crops for climate change mitigation through deployment for enhanced weathering. *Biol Lett*. 2017 Apr;13(4):20160714.
24. Swoboda P, Döring TF, Hamer M. Remineralizing soils? The agricultural usage of silicate rock powders: A review. *Science of The Total Environment*. 2022 Feb;807:150976.

25. Te Pas EEEM, Hagens M, Comans RNJ. Assessment of the enhanced weathering potential of different silicate minerals to improve soil quality and sequester CO<sub>2</sub>. *Front Clim.* 2023 Jan 10;4:954064.
26. Van Straaten P. Farming with rocks and minerals: challenges and opportunities. *An Acad Bras Ciênc.* 2006 Dec;78(4):731–47.
27. Grover SP, Butterly CR, Wang X, Gleeson DB, Macdonald LM, Tang C. Liming and priming: the long-term impact of pH amelioration on mineralisation may negate carbon sequestration gains. *Soil Security.* 2021 Jun 1;3:100007.
28. Paradelo R, Virto I, Chenu C. Net effect of liming on soil organic carbon stocks: A review. *Agriculture, Ecosystems & Environment.* 2015 Apr;202:98–107.
29. Paessler D, Steffens R, Hammes J, Smet I. Insights from monitoring leachate alkalinity, pCO<sub>2</sub> and CO<sub>2</sub> efflux of 400 weathering experiments over one year. *Carbon Drawdown Initiative*; 2024.
30. Yan Y, Dong X, Li R, Zhang Y, Yan S, Guan X, et al. Wollastonite addition stimulates soil organic carbon mineralization: Evidences from 12 land-use types in subtropical China. *CATENA.* 2023 May;225:107031.
31. Dietzen C, Harrison R, Michelsen-Correa S. Effectiveness of enhanced mineral weathering as a carbon sequestration tool and alternative to agricultural lime: An incubation experiment. *International Journal of Greenhouse Gas Control.* 2018 Jul;74:251–8.
32. Buss W, Hasemer H, Ferguson S, Borevitz J. Stabilisation of soil organic matter with rock dust partially counteracted by plants. *Global Change Biology.* 2024 Jan;30(1):e17052.
33. Xu T, Yuan Z, Vicca S, Goll DS, Li G, Lin L, et al. Enhanced silicate weathering accelerates forest carbon sequestration by stimulating the soil mineral carbon pump. *Global Change Biology.* 2024;30(8):e17464.
34. Davidson EA, Janssens IA. Temperature sensitivity of soil carbon decomposition and feedbacks to climate change. *Nature.* 2006 Mar;440(7081):165–73.
35. Lehmann J, Kleber M. The contentious nature of soil organic matter. *Nature.* 2015 Dec;528(7580):60–8.
36. Rovira A, Greacen E. The effect of aggregate disruption on the activity of microorganisms in the soil. *Australian Journal of Agricultural Research.* 1957;8(6):659.
37. Hartley IP, Hill TC, Chadburn SE, Hugelius G. Temperature effects on carbon storage are controlled by soil stabilisation capacities. *Nat Commun.* 2021 Nov 18;12(1):6713.
38. Orchard VA, Cook FJ. Relationship between soil respiration and soil moisture. *Soil Biology and Biochemistry.* 1983 Jan;15(4):447–53.
39. Ramesh T, Bolan NS, Kirkham MB, Wijesekara H, Kanchikerimath M, Srinivasa Rao C, et al. Soil organic carbon dynamics: Impact of land use changes and management practices: A review. In: *Advances in Agronomy* [Internet]. Elsevier; 2019 [cited 2024 Oct 29]. p. 1–107. Available from: <https://linkinghub.elsevier.com/retrieve/pii/S0065211319300343>

40. Gabriel CE, Kellman L. Investigating the role of moisture as an environmental constraint in the decomposition of shallow and deep mineral soil organic matter of a temperate coniferous soil. *Soil Biology and Biochemistry*. 2014 Jan;68:373–84.
41. Balesdent J, Chenu C, Balabane M. Relationship of soil organic matter dynamics to physical protection and tillage. *Soil and Tillage Research*. 2000 Feb 1;53(3):215–30.
42. Besnard E, Chenu C, Balesdent J, Puget P, Arrouays D. Fate of particulate organic matter in soil aggregates during cultivation. *European J Soil Science*. 1996 Dec;47(4):495–503.
43. Chevallier T, Blanchart E, Alain A, Feller C. The physical protection of soil organic carbon in aggregates: A mechanism of carbon storage in a Vertisol under pasture and market gardening (Martinique, West Indies). *Agriculture, Ecosystems & Environment*. 2004 Jul 1;103:375–87.
44. Six J, Elliott E t., Paustian K, Doran JW. Aggregation and Soil Organic Matter Accumulation in Cultivated and Native Grassland Soils. *Soil Science Society of America Journal*. 1998;62(5):1367–77.
45. Allen Hammer P, Langhans RW. Experimental Design Considerations for Growth Chamber Studies1. *hortsc*. 1972 Oct;7(5):481–3.
46. Crop Science Society of America. *Controlled Environment Research Guidelines for Researchers and Reviewers*. Crop Science Society of America. 2008;
47. Lee C, Rawlings JO. Design of Experiments in Growth Chambers — Uniformity Trials in the North Carolina State University Phytotron 1. *Crop Science*. 1982 May;22(3):551–8.
48. Bunce JA. Low humidity effects on photosynthesis in single leaves of C4 plants. *Oecologia*. 1982 Aug;54(2):233–5.
49. Bunce JA. Effects of Humidity on Photosynthesis. *J Exp Bot*. 1984;35(9):1245–51.
50. Cowan IR. Stomatal Behaviour and Environment. In: Preston RD, Woolhouse HW, editors. *Academic Press*; 1978. p. 117–228. (*Advances in Botanical Research*; vol. 4). Available from: <https://www.sciencedirect.com/science/article/pii/S0065229608603705>
51. Rawson HM, Begg JE, Woodward RG. The effect of atmospheric humidity on photosynthesis, transpiration and water use efficiency of leaves of several plant species. *Planta*. 1977;134(1):5–10.
52. Lewis J, Sjöstrom J. Optimizing the experimental design of soil columns in saturated and unsaturated transport experiments. *Journal of Contaminant Hydrology*. 2010 Jun;115(1–4):1–13.
53. Poorter H, Fiorani F, Pieruschka R, Wojciechowski T, Putten WH, Kleyer M, et al. Pampered inside, pestered outside? Differences and similarities between plants growing in controlled conditions and in the field. *New Phytol*. 2016 Dec;212(4):838–55.
54. Burns JH, Anacker BL, Strauss SY, Burke DJ. Soil microbial community variation correlates most strongly with plant species identity, followed by soil chemistry, spatial location and plant genus. *AoB PLANTS*. 2015 May 1;7(0):plv030–plv030.

55. Chiaravalloti I, Theunissen N, Zhang S, Wang J, Sun F, Ahmed AA, et al. Mitigation of soil nitrous oxide emissions during maize production with basalt amendments. *Front Clim.* 2023 Jun 22;5:1203043.
56. Renforth P, Pogge von Strandmann PAE, Henderson GM. The dissolution of olivine added to soil: Implications for enhanced weathering. *Applied Geochemistry.* 2015 Oct 1;61:109–18.
57. Amann T, Hartmann J, Struyf E, de Oliveira Garcia W, Fischer EK, Janssens I, et al. Enhanced Weathering and related element fluxes – a cropland mesocosm approach. *Biogeosciences.* 2020 Jan 8;17(1):103–19.
58. Buckingham FL, Henderson GM, Holdship P, Renforth P. Soil core study indicates limited CO<sub>2</sub> removal by enhanced weathering in dry croplands in the UK. *Applied Geochemistry.* 2022 Dec;147:105482.
59. Kelland ME, Wade PW, Lewis AL, Taylor LL, Sarkar B, Andrews MG, et al. Increased yield and CO<sub>2</sub> sequestration potential with the C<sub>4</sub> cereal *Sorghum bicolor* cultivated in basaltic rock dust-amended agricultural soil. *Glob Change Biol.* 2020 Jun;26(6):3658–76.
60. Kanzaki Y, Planavsky N, Zhang S, Jordan J, Reinhard CT. Soil cation storage as a key control on the timescales of carbon dioxide removal through enhanced weathering. 2024 Mar; Available from: <http://dx.doi.org/10.22541/essoar.170960101.14306457/v1>
61. Integrated Crop Management. Iowa State University Extension and Outreach. 2017 [cited 2024 Oct 31]. How Fast and Deep do Corn Roots Grow in Iowa? | Integrated Crop Management. Available from: <https://crops.extension.iastate.edu/cropnews/2017/06/how-fast-and-deep-do-corn-roots-grow-iowa>
62. Eosense. Eosense: Application Article. 2020. Using the eosMX to Coordinate Automated Sampling from Soil Gas Wells. Available from: <https://eosense.com/application-article-using-the-eosmx-recirculating-multiplexer-with-manual-chambers/>
63. Eosense. Eosense: eosAC-LT/LO Application Article. 2022. Measuring Net Ecosystem Exchange with the eosAC-LT/LO. Available from: <https://eosense.com/measuring-nee/>
64. Anthony TL, Silver WL. Field Deployment of Picarro G2508 and Eosense eosAC/eosMX in Perennially or Periodically Flooded Soils. Eosense Application Note AN041 [Internet]. 2020 May; Available from: [https://www.picarro.com/environmental/an041\\_field\\_deployment\\_of\\_picarro\\_g2508\\_and\\_eosense\\_eosaceosmx\\_in\\_perennially\\_or#:~:text=Here%20we%20report%20on%20modifications%20to%20a%20system,Plastics%29%20for%20continuous%20measurements%20in%20periodically%20inundated%20fields.](https://www.picarro.com/environmental/an041_field_deployment_of_picarro_g2508_and_eosense_eosaceosmx_in_perennially_or#:~:text=Here%20we%20report%20on%20modifications%20to%20a%20system,Plastics%29%20for%20continuous%20measurements%20in%20periodically%20inundated%20fields.)
65. Haque F, Santos RM, Chiang YW. CO<sub>2</sub> sequestration by wollastonite-amended agricultural soils – An Ontario field study. *International Journal of Greenhouse Gas Control.* 2020 Jun;97:103017.
66. Basile-Doelsch I, Balesdent J, Pellerin S. Reviews and syntheses: The mechanisms underlying carbon storage in soil. *Biogeosciences.* 2020 Oct 30;17(21):5223–42.

**Table 1:** Cumulative Average CO<sub>2</sub> Emissions from Run 1 and Run 2

Iteration	Application	Mean cumulative CO <sub>2</sub> emissions (mmol/m <sup>2</sup> )	Standard deviation (1σ)
Run 1	5 tons basalt/acre	2909.68	1052.43
	Control	2569.34	751.82
Run 2	5 tons basalt/acre	2205.08	1023.46
	Control	2662.89	392.37

**Table 2:** Comparison of Means from Run 1 and Run 2 with a t-test

Iteration	Group 1	Group 2	t-value	p-value
Run 1	Basalt	Control	0.526	0.613
Run 2	Basalt	Control	-0.835	0.428

**Table 3:** Average TOC content (weight %) of control and basalt amended containers over time.

Date	07/27/22	08/01/22	08/29/22	10/10/22	All post amendment time
Average TOC (%) Basalt	2.39	2.61	2.46	2.55	2.54
Average TOC (%) Control	2.58	2.33	2.30	2.47	2.37
Stdev TOC (%) Basalt (1σ)	0.32	0.18	0.13	0.22	0.19
Stdev TOC (%) Control (1σ)	0.20	0.16	0.17	0.10	0.17

**Table 4:** Average total carbon (TC) content (weight %) of control and basalt amended containers over time.

Date	07/27/22	08/01/22	08/29/22	10/10/22	All post amendment time
Average TC (%) Basalt	2.39	2.64	2.49	2.56	2.54
Average TC (%) Control	2.58	2.33	2.30	2.47	2.37
Stdev TC (%) Basalt (1σ)	0.32	0.18	0.12	0.22	0.19
Stdev TC (%) Control (1σ)	0.20	0.16	0.17	0.10	0.17

**Table 5:** p-values from t-test of differences of means in percent carbon stocks by weight between control and basalt amended containers. Bolded values are statistically significant (p-value below 0.05).

	7/27/2022	8/1/2022	8/29/2022	10/10/2022	All post amendment time
TOC	0.348	<b>0.049</b>	0.175	0.565	<b>0.018</b>
TIC	0.347	<b>0.004</b>	<b>0.014</b>	<b>0.026</b>	<b>0.000</b>
TC	0.348	<b>0.035</b>	0.102	0.483	<b>0.007</b>

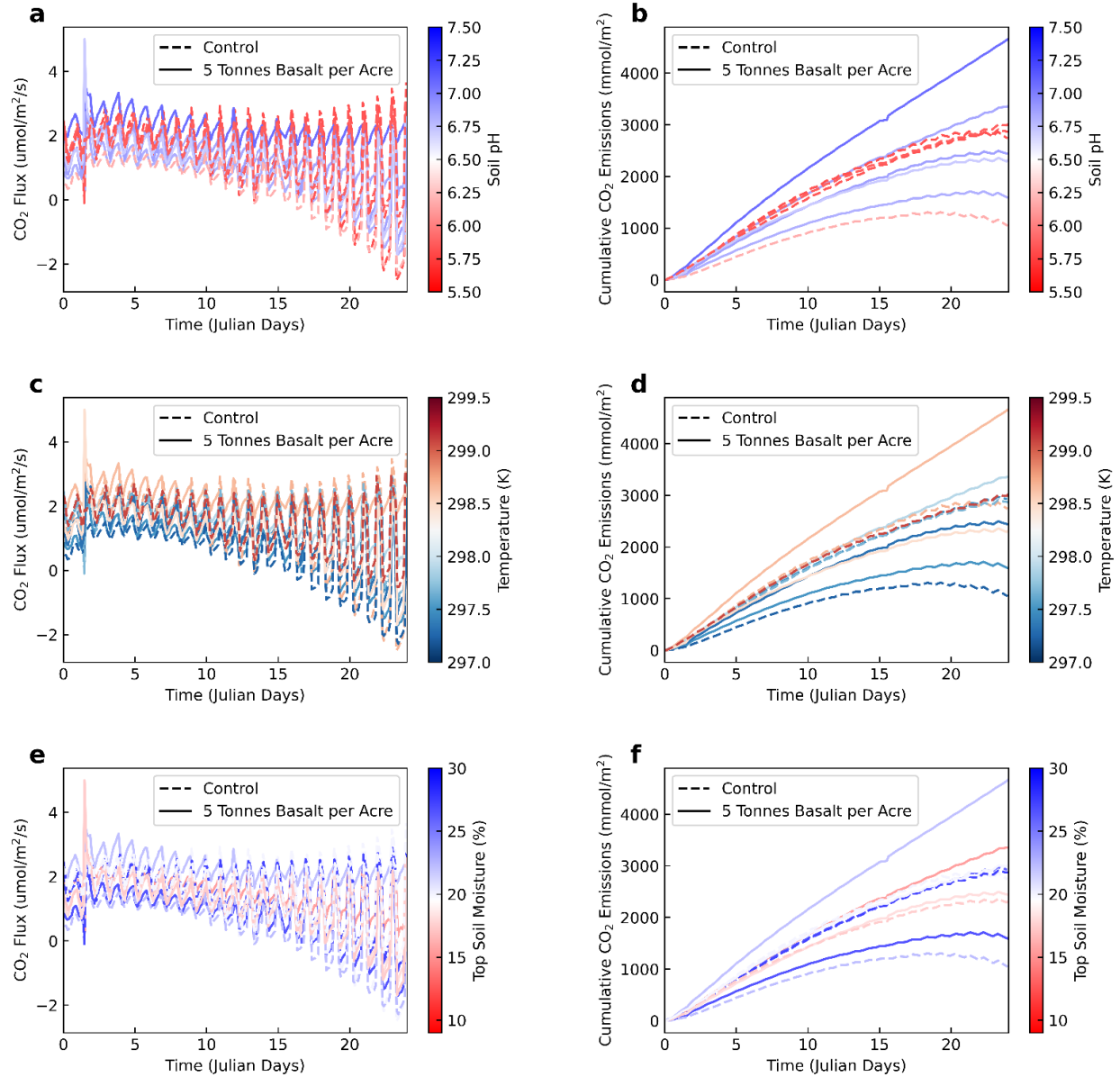


Figure 1: (a, c, e) CO<sub>2</sub> fluxes (μmol/m<sup>2</sup>/s) and (b, d, f) cumulative CO<sub>2</sub> emissions (mmol/m<sup>2</sup>) relative to days (from start of Run 1) color coded by (a, b) pH, (c, d) temperature (K), and (e, f) top soil moisture (%VWC). The dashed lines represent control containers, and the solid lines represent basalt amended containers.

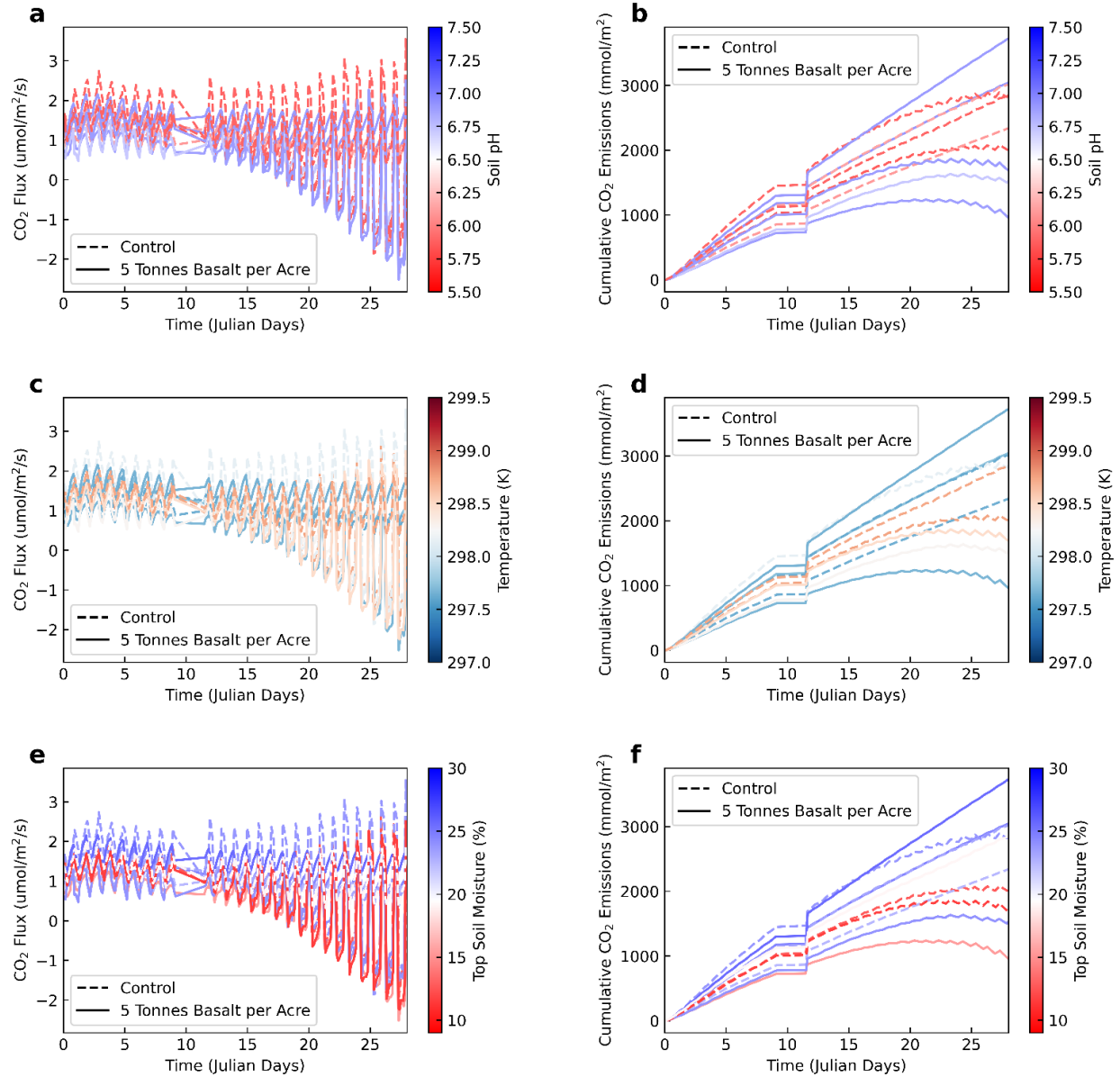


Figure 2: (a, c, e) CO<sub>2</sub> fluxes ( $\mu\text{mol}/\text{m}^2/\text{s}$ ) and (b, d, f) cumulative CO<sub>2</sub> emissions ( $\text{mmol}/\text{m}^2$ ) relative to days (from start of Run 2) color coded by (a, b) pH, (c, d) temperature (K), and (e, f) top soil moisture (%VWC). The dashed lines represent control containers, and the solid lines represent basalt amended containers. The 2.5-day gap in measurements between early on Day 9 to midday on Day 11 was caused by a software crash.



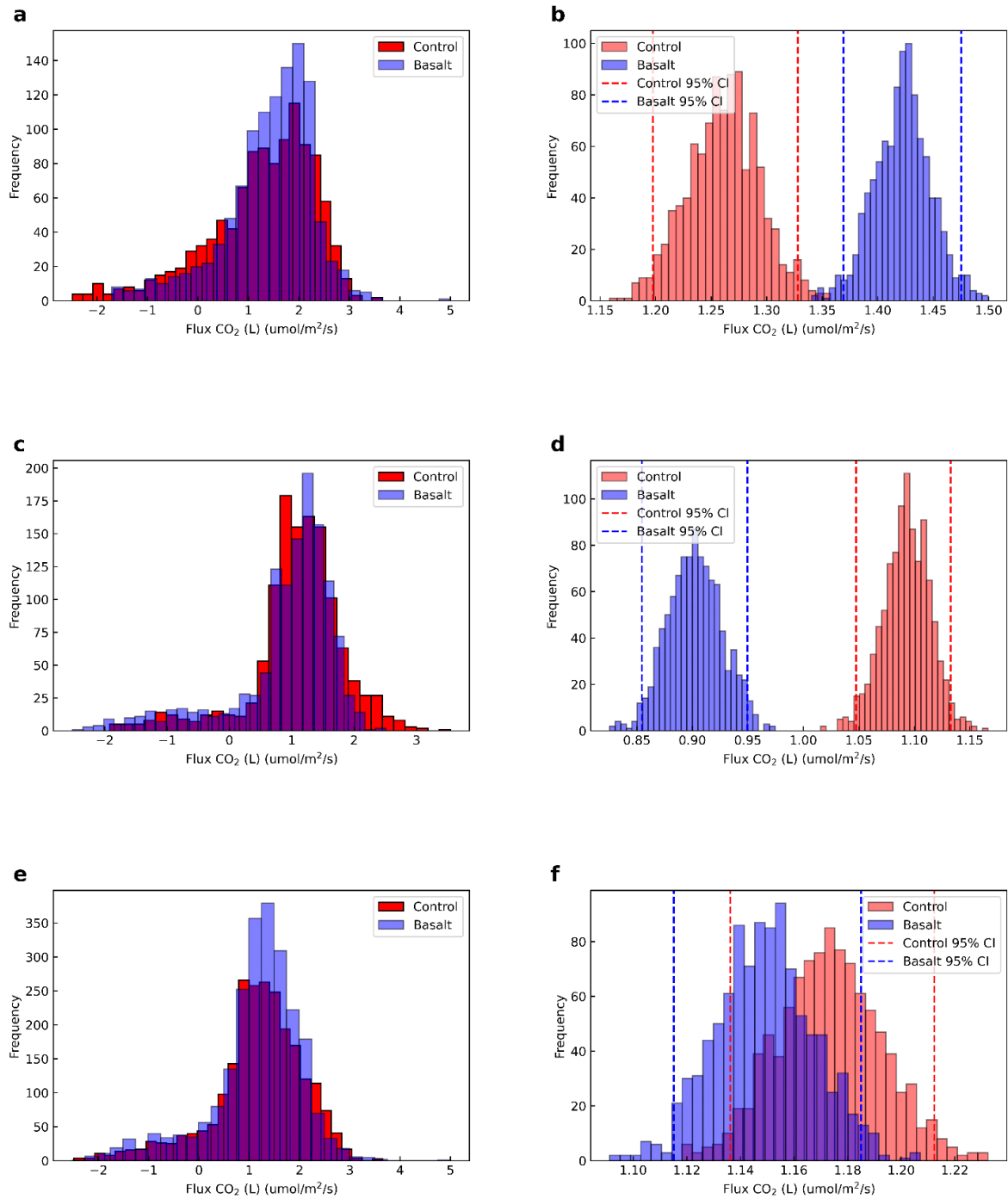


Figure 3: Histogram showing the frequency of CO<sub>2</sub> fluxes ( $\mu\text{mol}/\text{m}^2/\text{s}$ ) of control (red) vs. basalt (blue) in (a) Run 1 and (c) Run 2 (e) Runs 1 and 2 combined. Histogram showing the distribution of bootstrap resampled means ( $n=1000$ ) for CO<sub>2</sub> fluxes ( $\mu\text{mol}/\text{m}^2/\text{s}$ ) from control (red) vs. basalt (blue) samples in (b) Run 1 (d) Run 2 (f) Runs 1 and 2 combined.

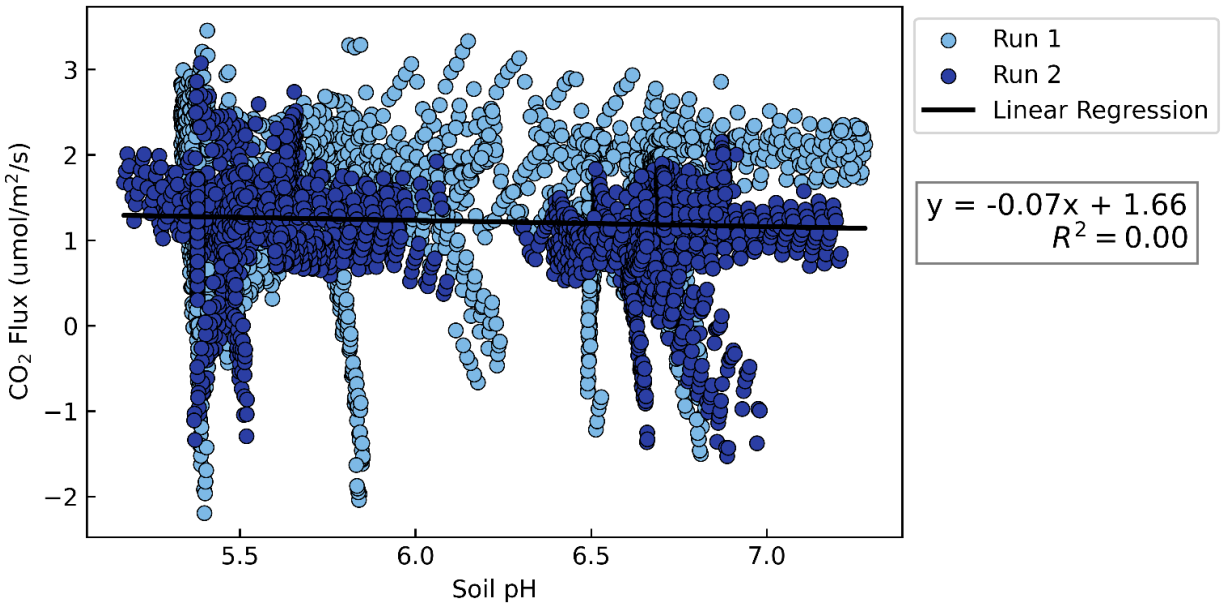


Figure 4: Crossplot showing all CO<sub>2</sub> fluxes (μmol/m<sup>2</sup>/s) as a function of soil pH for Run 1 (light blue) and Run 2 (dark blue). A linear regression is shown in black for the combined data ( $y = -0.07x + 1.66$ ,  $R^2 = 0.00$ ).

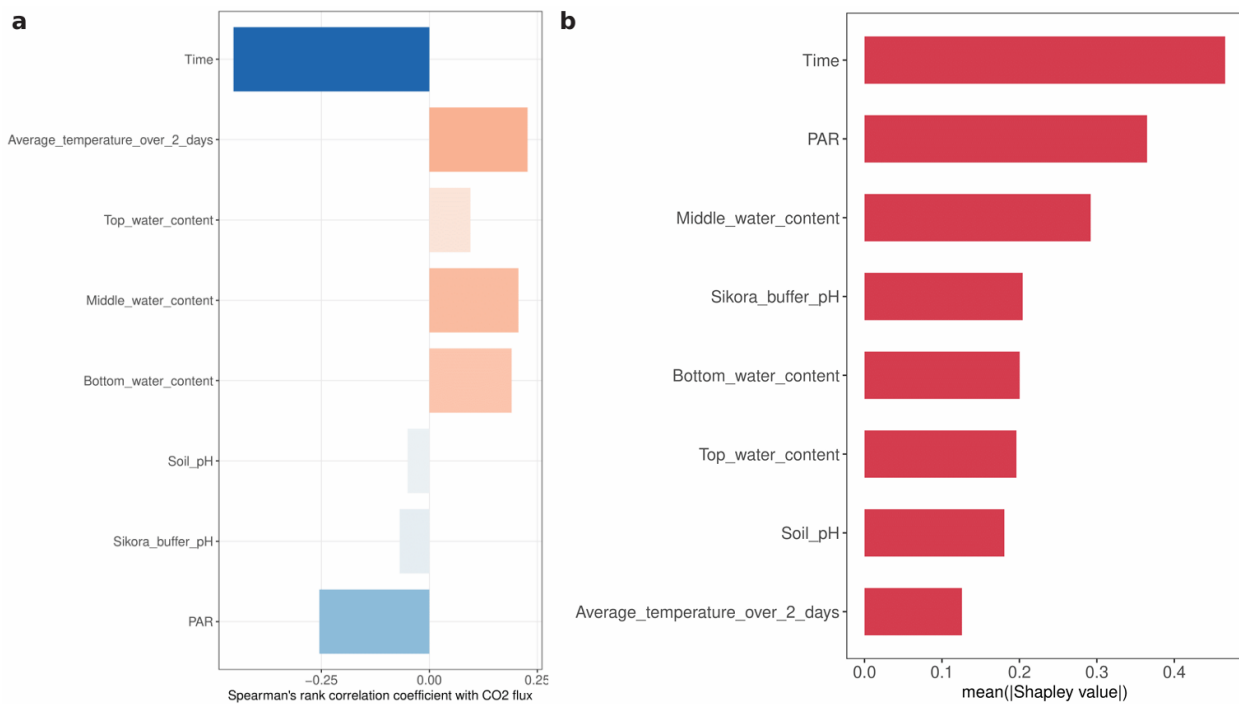


Figure 5: (a) Spearman's rank correlation plot for each measurement (from Runs 1 and 2 combined). (b) Permutation importance figure showing the relative importance of levers on CO<sub>2</sub> fluxes revealed by the RF framework.

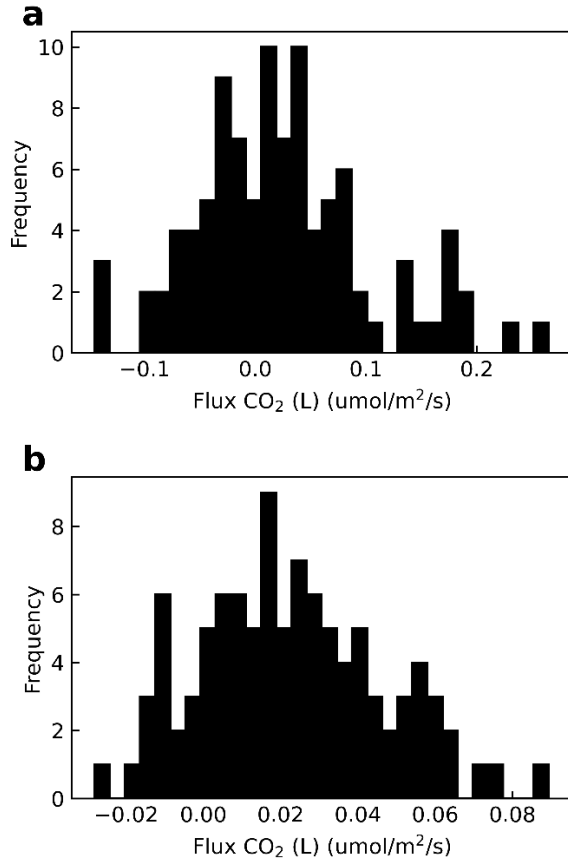


Figure 6: The distribution of differences in average CO<sub>2</sub> flux between control and basalt amended containers (i.e., average CO<sub>2</sub> flux<sub>control</sub> – average CO<sub>2</sub> flux<sub>basalt</sub>) when a) 90% of samples are removed and b) 50% of samples are removed. n=100 resamplings.

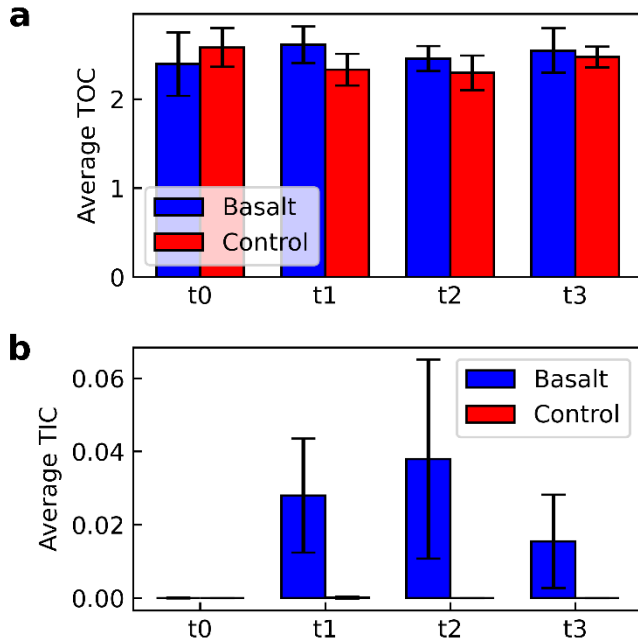


Figure 7: A bar graph showing the average carbon stock values: (a) TOC and (b) TIC for basalt vs. control at the four timesteps (t0 = 7/27/22, t1 = 8/1/22, t2 = 8/29/22, t3 = 10/10/22). Basalt is shown in blue, and control is shown in red. Error bars indicate standard deviation from the mean ( $1\sigma$ ).